ResearchGate

See discussions, stats, and author profiles for this publication at: https://www.researchgate.net/publication/233783338

Linear Viscoelastic Response of Dendronized Polymers

ARTICLE *in* MACROMOLECULES · NOVEMBER 2012

Impact Factor: 5.8 · DOI: 10.1021/ma301029t

CITATIONS
9

READS
65

9 AUTHORS, INCLUDING:

Baozhong Zhang
Lund University
29 PUBLICATIONS **379** CITATIONS
SEE PROFILE

Reinhard Sigel
The German University in Cairo
42 PUBLICATIONS **833** CITATIONS
SEE PROFILE

Oscar Bertran
Polytechnic University of Catalonia
43 PUBLICATIONS **303** CITATIONS
SEE PROFILE

Carlos Alemán
Polytechnic University of Catalonia
462 PUBLICATIONS **6,036** CITATIONS
SEE PROFILE

Available from: Baozhong Zhang
Retrieved on: 02 February 2016

Macromolecules

Article

pubs.acs.org/Macromolecules

Linear Viscoelastic Response of Dendronized Polymers

R. Pasquino,*[,†] B. Zhang,[‡] R. Sigel,[§] H. Yu,[‡] M. Ottiger,[‡] O. Bertran,[∥] C. Aleman,[⊥,#] A. D. Schlüter,[‡] and D. Vlassopoulos[†,%]

[†]Institute of Electronic Structure and Laser, Foundation for Research and Technology (FORTH), 71110 Heraklion, Crete, Greece

[‡]Department of Materials, Institute of Polymers, Swiss Federal Institute of Technology (ETH), 8093 Zurich, Switzerland

[§]Adolphe Merkle Institute, University of Fribourg, 1723 Marly, Switzerland

[∥]Departament of Applied Physics, Universitat Politècnica de Catalunya, EEI, Pça Rei 15, Igualada 08700, Spain

[⊥]Universitat Politècnica de Catalunya, Department of Chemical Engineering, ETSEIB, Diagonal 647, 08028 Barcelona, Spain

[#]Centre for Research in Nano-Engineering, Universitat Politècnica de Catalunya, Edifici C′, C/Pasqual i Vila s/n, Barcelona E-08028, Spain

[%]Department of Materials Science & Technology, University of Crete, 71003 Heraklion, Crete, Greece

ABSTRACT: We investigate the linear rheology of well-defined dendronized polymers (DPs). They consist of polymethacrylate backbones with tree-like branches (dendrons) of different generations, from zeroth to fourth, grafted at each monomer and a methyleneoxycarbonyl spacer between the polymerizable group and the dendritic substituent. The degrees of polymerization for the different generation polymers are almost constant, allowing for systematic studies as a function of generation. Because of the synthetic approach, these macromolecules possess *tert*-butoxycarbonyl (Boc) groups which promote hydrogen bonding, whereas the benzene groups allow for weaker bonding (π-stacking) as well. The master curves of frequency-dependent storage and loss moduli of these macromolecular structures were obtained via time−temperature superposition of dynamic frequency sweeps at various temperatures. To access slow relaxations, creep measurements were performed at long times and converted to frequency-dependent moduli. For the first generation, it was possible to detect relaxation processes suggesting an approach to the terminal regime (flow). On the other hand, the zeroth and second to fourth generation polymers exhibited a solid-like behavior throughout a wide range of frequencies. The fast relaxations reflect the coupling of segmental friction and hydrogen bonding and render the WLF-type analysis nontrivial. On the basis of the molecular structure of these unique materials as revealed by molecular dynamics simulations and complementary studies with their linear analogues poly(methyl methacrylate) and poly(*tert*-butyl)methacrylate, we propose that DPs resemble weakly interpenetrating elongated core−shell systems. As generation increases, their enhanced rigidity and intermolecular hydrogen bonding, which occurs primarily toward the outer surface of the DPs, appear to dominate the dynamics. PG0 is not a DP and has an open structure that promotes intermolecular bonding. These results provide design guidelines for ultrahigh-molecular-weight responsive polymers with possibilities for multifunctional substitution and tailoring Frheological response from liquid-like to solid-like.

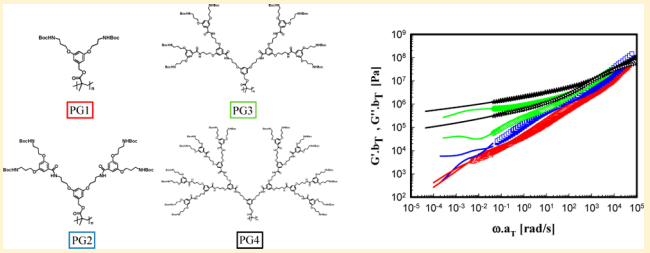

I. INTRODUCTION

It is well-known that macromolecular architecture greatly affects the rheological properties of polymer materials.[1] A unique class of polymers reflecting such effects and having potential for a great deal of applications are dendritic macromolecules, and as such they have received a lot of attention recently.[2−5] They are typically synthesized via step-controlled synthesis, and their polymeric nature pertains to their repetitive structure made of monomers. Whereas the chemistry of these special branched materials has matured over the past 20 years[2,6−10] and a large number of different dendritic families of different generations can be synthesized, albeit not always in a straightforward manner, the details of their rheological response, which governs their final properties in applications, remain elusive. From the limited rheological studies available, the linear viscoelastic response becomes more complex and moves from viscoelastic liquid to viscoelastic solid as the generation increases.[4,5,9] In general, dendritically branched polymers with large segments between branches (having molar masses well above the entanglement limit), often called Cayley-tree polymers (see Figure 1), relax their stress hierarchically, from the outer to the inner portions of the molecular structure.[1,11−13] Their structure is regular (symmetric growth of branching with generation) in contrast to

Received: May 20, 2012
Revised: October 4, 2012
Published: October 29, 2012

ACS Publications © 2012 American Chemical Society

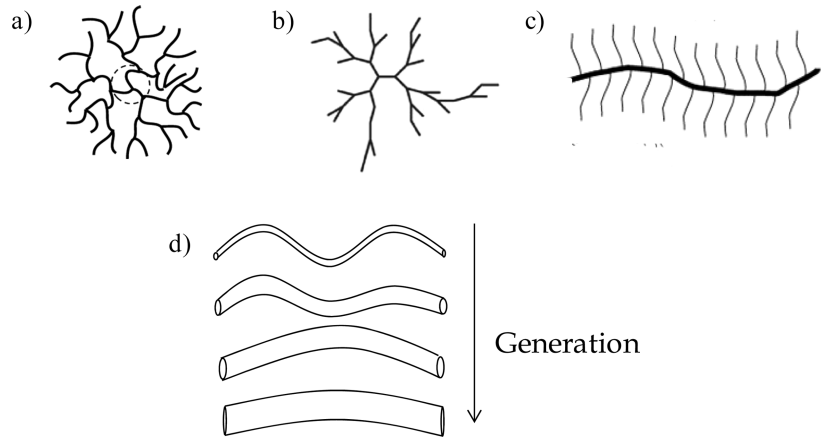

Figure 1. Schematic illustration of the molecular conformations of different branched macromolecular structures: (a) dendritically branched polymers of the Cayley-tree type; (b) hyperbranched polymers; (c) bottlebrushes; (d) dendronized polymers with increasing generation number in the direction of the arrow (see text). The cartoons are not drawn to scale.

irregular (albeit similar) hyperbranched polymers. As the relaxation proceeds inward, the relaxed portions act as solvents for the remaining entanglements of the inner structure (dynamic tube dilation, DTD), eventually speeding-up relaxation.[12,13] Despite a number of subtle issues, this naive description is fairly accurate.[1,12−14] However, when the segments molar masses are below the entanglement limit, this framework does not work and the dendrimer response is often self-similar.[4]

Driven by both scientific and technological challenges, synthetic chemists incorporate functional groups in macromolecules. Often we can take advantage of hydrogen bonding, which provides a route for reversibly linking segments in solution or in the melt. They result in the formation of transient networks[15] or supramolecular assemblies,[16] with interesting albeit complex and tunable rheological properties. This is a huge area with immense opportunities in materials design but with many formidable challenges in the understanding of their properties. Of particular significance and potential impact is the combination of bonding with well-defined dendritic structures for tailoring the rheology.

Here, we focus our attention on controlled dendronized polymers[5,8−10] (DPs), where each repeat unit of a linear backbone carries a perfectly branched dendron (tree) with very small segments (typically monomers) between branches. Their typical structure perfection exceeds 98%. While Cayley-tree and hyperbranched polymers attain an approximately spherical shape, dendronized polymers can be better visualized as "sausages", i.e., highly elongated structures (Figure 1). There are important details on the effect of generation which will be elucidated later, but here we wish to make the contrast between spherical dendritically/hyperbranched and elongated dendronized conformations. In such cases, the above-mentioned hierarchical concept is not applicable, at least in a straightforward way, and the dynamics is controlled by the topological interactions at the scale of the "sausage", fluctuations of outer segments, and possible interactions of intramolecular and, more importantly, intermolecular nature. Hence, new phenomena and physical properties may result from the unusual architecture of dendritic macromolecules, in comparison to linear polymers. There are several systematic rheological studies on well-defined dendritic and bottlebrush-type polymers[3,4,17−21] but only limited studies on dendronized polymers.[5,10] Note that the highly branched nature of the latter macromolecular structures affects their glass transition temperature (T_g) via the many free dangling ends (which lower T_g) and the steric constraints via the number of branch points (which increase T_g).[5,22−24] Note that the bottlebrush polymers, often called polymacromonomers, are much simpler than DPs since each monomer has just a linear side chain as branch (Figure 1). In the true-bottlebrush limit when the side chains are too short, they could be thought as having "sausage"-like conformations albeit more flexible than DPs. In the melt state they exhibit an unusually small low-frequency plateau modulus (typically of the order of 1 kPa), apparently reflecting topological interactions at the scale of the whole macromolecule, resulting in the temporary trapping of the densely branched entangled backbones which eventually flow as a colloid-like objects. The possible interpenetration of the densely grafted side chains is very weak, and there is no bonding of any sort formed; hence, the related relaxation is fast and self-similar. Because of the low plateau modulus, they are also called supersoft elastomers.

Recent advances in organic chemistry have led to the model synthesis of well-defined long dendronized polymers whose backbone monomers are linked to dendrons.[5,7,8,25] A variety of dendronized polymeric structures are now available.[26] DPs represent a special and novel class of regularly highly branched linear polymers with ultrahigh total molar mass, where the high-density layer around the backbone influences their conformation and rigidity. Naturally, the generation of the dendron affects the rigidity. To a first approach, keeping the coarse picture of "sausage" conformation, with increasing generation the macromolecule becomes more rigid.[8,27,28] This is illustrated in the cartoon of Figure 1 and is supported by molecular dynamics (MD) simulations.[29] This point is considered as central to the topological interactions and dynamics of DPs and will be further discussed below. Clearly, elucidating the rheological response of these intriguing macromolecules with ultrahigh total molecular weight and a range of potential applications[8,25] is a formidable challenge.

In this work we present a detailed rheological study, complemented by calorimetric information, of high-molar-mass, zeroth- to fourth-generation dendronized polymers. Because of the mode of synthesis,[5,8] the representatives of this series have almost the same degree of polymerization and

dx.doi.org/10.1021/ma301029t | Macromolecules 2012, 45, 8813−8823

molar mass distribution. This allows a systematic, generation-dependent study of glass transition and viscoelasticity. This combination of techniques can be used as analytical probe for the morphological structure of this series of polymers and for designing structures with desired properties.

The paper is organized as follows: The experimental section II includes the materials and methods used whereas the results are presented and discussed in section III. Finally, section IV summarizes the key conclusions.

II. EXPERIMENTS AND SIMULATIONS

II.1. Materials. The homologous series of methacrylate-based dendronized polymers of different generations was obtained from the first-generation PG1, which was subjected to repeated deprotection/dendronization reactions as described elsewhere.[5,24] The synthesis was carried out so as to have the least possible impact on main chain length and distribution. The molar masses and (rather high) polydispersities are listed in Table 1. The structure perfection was quantified to be close to 100% for each step, resulting in overall perfection for PG4 of >98%. PG0 was synthesized independently according to the literature procedure.[30,31] The procedure and analytical details are provided in section II.1.1. Figure 2 illustrates the chemical structures of the four generations along with PG0 and some linear polymers used (see below). Based on the molecular details depicted, these polymers in the melt exhibit in principle two types of molecular interactions: (a) hydrogen bonding between the protons on the NH groups (the amido groups) and mainly the oxygen atoms in the ether groups and the amide groups; (b) association of the aromatic rings via π,π-stacking, which results in weaker and shorter range bonds. Since the role of hydrogen bonding is central to the interpretation of this work, we note that whereas there is evidence of the existence of hydrogen bonds (from NMR spectroscopy), a detailed quantitative study is a far nontrivial matter. In addition, there is not yet direct evidence of inter- vs intramolecular hydrogen bonds other than MD simulations. Further experimental evidence is the subject of future studies.

Table 1. Molecular Characteristics of the Samples Used

sample code	$M_n \times 10^{-6}$ [g/mol]	PDI	DP_n
PMMA	0.26	1.04	2653
PtBMA	0.29	1.04	2042
PG0	0.26	7.4	1100
PG1	0.59	5.03	1129
PG2	1.29	3.30	1058
PG3	2.58	3.69	982
PG4	6.26	3.08	1153

The samples were molded overnight at 110 °C, in a homemade mold under vacuum, in order to eliminate humidity and to shape them as needed for rheological measurements (e.g., to avoid trimming while loading in the rheometer). In the case of PG0, the sample was annealed for about 1 week at 110 °C to remove traces of dioxane trapped in it and ensure thermal equilibration (as judged from the time-independent rheological measurements discussed below). In order to confirm that this annealing did not affect the chemical structure (and hence the rheological behavior) of the samples in any possible way, sample PG4 was treated thermally, following both procedures, i.e., overnight and week-long annealing. The resulting rheological response was identical in the two cases. As discussed later, the longer annealing needed for PG0 is attributed to strong hydrogen bonding which has a strong intermolecular character due to the molecule's open structure (it leads to denser intermolecular packing compared to higher generations).

Commercial poly(methyl methacrylate) (PMMA) and poly(*tert*-butyl methacrylate) (PtBMA) (from Polymer Standards Service, Germany) were also measured as reference materials for comparison with the linear backbone of the homologous DP series. The molar masses were chosen to be similar to PG0. Details are shown in Table 1. These samples were molded at 180 °C for 3 h under vacuum. Before the molding, the PtBMA sample was annealed at 220 °C for about 1 h to remove traces of solvent trapped in the structure. Examining the molecular structures of Figure 2, we note that the PG0 polymer differs from the PtBMA by the presence of a much crowded substituent, containing an amido group.

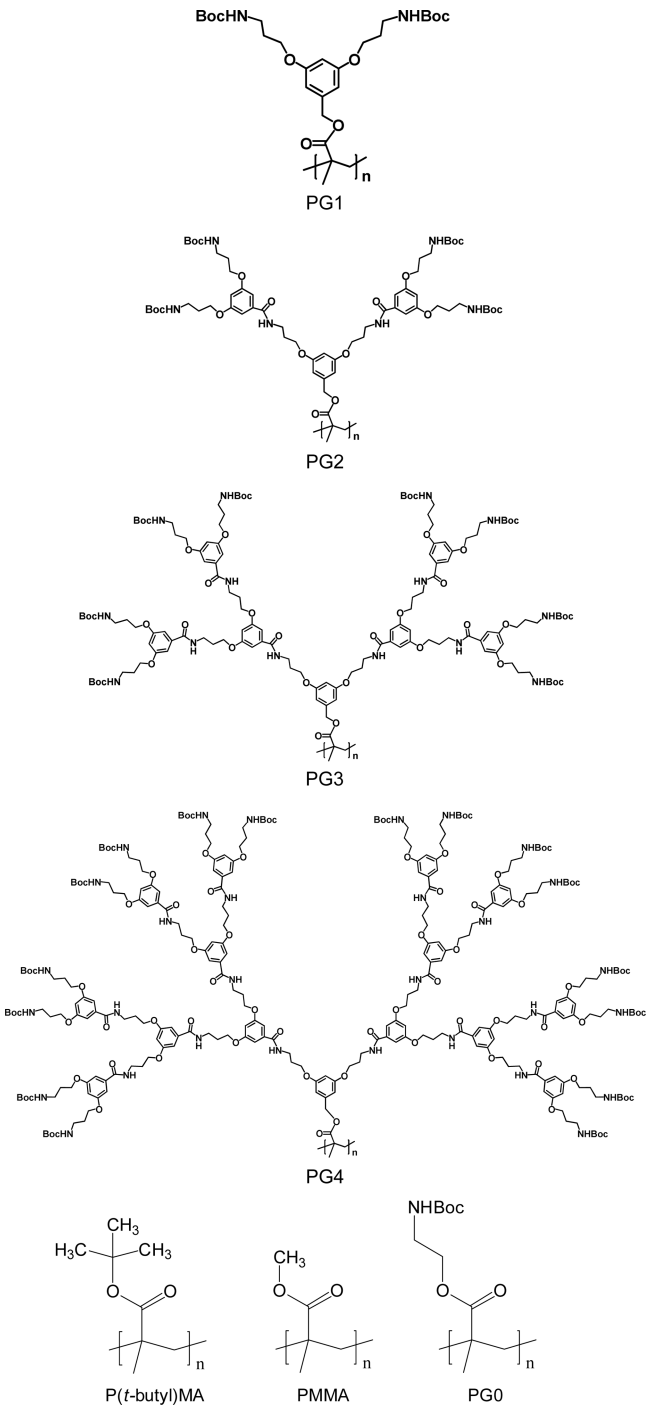

Figure 2. Molecular structure of the different polymers used in this work.

II.1.1. Synthesis of PG0. N-(tert-Butoxycarbonyl)ethanolamine.[30] A solution of di-*tert*-butyl dicarbonate (38.20 g, 175.0 mmol, 1.06 equiv) in dichloromethane (DCM, 6 mL) was added dropwise to a solution of ethanolamine (10.08 g, 165.0 mmol, 1 equiv) in DCM (210 mL) and stirred for 5 h at room temperature. The reaction solution was washed with saturated $NaHCO_3$ (3 × 200 mL), dried

dx.doi.org/10.1021/ma301029t | Macromolecules 2012, 45, 8813−8823

Scheme 1. Synthetic Route of PG0

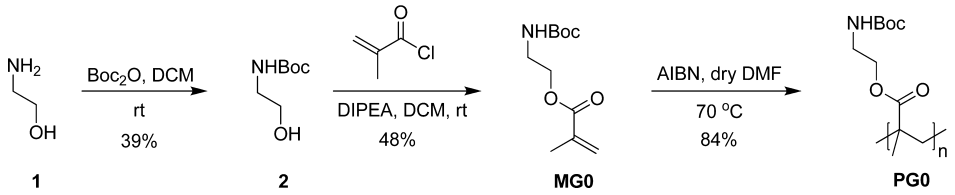

over $MgSO_4$ and concentrated *in vacuo*. The obtained crude mixture was distilled under reduced pressure to give *N*-(*tert*-butoxycarbonyl)-ethanolamine (10.74 g, 39%). ^{1}H NMR ($CDCl_3$, 300 MHz): 3.70 (t, 2H, CH_2OH); 3.29 (t, 2H, CH_2NH); 1.45 (s, 9H, NH*Boc*).

2-(tert-Butoxycarbonylamino)ethyl Methacrylate.[31] Methacryloyl chloride (1.45 g, 13.9 mmol, 1.12 equiv) was added to a solution of *N*-(*tert*-butoxycarbonyl)ethanolamine (1.99 g, 12.4 mmol, 1 equiv) and *N*,*N*-diisopropylethylamine (3.24 mL, 18.6 mmol, 1.50 equiv) in anhydrous DCM (20 mL) at 0 °C. The reaction mixture was allowed to warm up to room temperature and stirred for 12 h. The red reaction solution was washed with water (10 mL), 10% citric acid (10 mL), 10% K_2CO_3 (10 mL), saturated $NaHCO_3$ (10 mL), and brine (10 mL). The organic layer was dried over Na_2SO_4, evaporated under reduced pressure, and crystallized from DCM/hexane to afford red crystals of 2-(*tert*-butoxycarbonylamino)ethyl methacrylate (1.35 g, 48%). ^{1}H NMR ($CDCl_3$, 300 MHz): 6.12 (s, 1H, (*H*)(H)C═CMe); 5.59 (s, 1H, (H)(*H*)C═CMe); 4.21 (t, 2H, O═COCH_2); 3.44 (m, 2H, CH_2NH); 1.95 (s, 3H, (H)(H)C═C*Me*); 1.45 (s, 9H, NH*Boc*).

PG0 (Scheme 1). A Schlenk flask was equipped with a stirring bar and flushed with N_2. Monomer 2-(*tert*-butoxycarbonylamino)ethyl methacrylate (1.02 g, 5.0 mmol) and AIBN (0.25 mL of 0.02 M AIBN solution in dry DMF, 0.005 mmol, 0.1 mol %) were added carefully to the bottom. The Schlenk flask was flushed with N_2 and evacuated several times. Dry DMF (1 mL) was added. The reaction was stirred gently at 70 °C for 24 h to afford a highly viscous gel. The reaction mixture was dissolved in DCM and purified by flash column chromatography (SiO_2, DCM). The obtained gel-like polymer was freeze-dried from dioxane to give PG0 as a white powder (0.86 g, 84%). ^{1}H NMR (DMSO-d_6, 300 MHz): 6.82 (br, s, 1H, N*H*); 3.85 (br, s, 2H, O═COCH_2); 3.17 (br, s, 2H, CH_2NH); 1.81 (br, s, 2H, C(CH_3)CH_2); 1.45 (s, 9H, NH*Boc*); 0.94−0.76 (br, m, 3H, C(CH_3)CH_2), GPC: $M_n \sim 206\,000$, $P_n \sim 1000$, PDI ∼ 3.1.

II.2. Differential Scanning Calorimetry (DSC). To detect the glass transition temperature (T_g) of these amorphous polymers, we performed DSC measurements with a PL-DSC calorimeter (Rheometric Scientific) with continuous flow of nitrogen gas in order to prevent any thermal degradation of the polymer. For PG1−PG4 the temperature ramp was from 20 to 100 °C, whereas for PG0 it was from 50 to 140 °C, and for PMMA and PtBMA it was from room temperature to 180 °C. The rate of heating (and cooling) was set for all the samples at 10 °C/min.

II.3. Rheology. Linear rheological measurements were performed using an ARES-2KFRTN1 strain-controlled rheometer (from TA, formerly Rheometric Scientific). Because of the limited quantities of samples available, we used invar (an alloy of copper and iron with very low thermal expansion coefficient) parallel plates with 8 mm plate diameter. The sample thickness ranged between 0.6 and 1 mm. Temperature control of ±0.1 °C was achieved with a convection oven operating with nitrogen gas to provide an inert atmosphere. For all samples, small-strain-amplitude oscillatory shear experiments (SAOS) were performed at different temperatures in order to create a master curve for the storage (G') and loss (G'') moduli over a broad frequency range using the principle of time−temperature superposition,[32] as detailed below. Before applying a frequency sweep, each sample was tested at each temperature to ensure thermal equilibration (via dynamic time sweeps) and determine the range of its linear viscoelastic response. The dynamic strain sweep tests were performed by sweeping the strain amplitude at fixed frequency, and the linear regime was determined by the independence of G' and G'' on strain. A temperature range from 70 to 120 °C was used for the homologous PG series. For PMMA and PtBMA the range was between 160 and 250 °C. In all cases, the lower temperature limit is set by the glass transition temperature (and relevant problems related to transducer compliance). On the other hand, the upper limit is set by the thermal stability of the samples (to prevent degradation). In particular, in the case of the PG series, the higher temperatures (exceeding 120 °C) were found to affect the stability of the Boc protecting groups.

Because of this upper temperature limit, in order to obtain reliable rheological data at as long relaxation times as possible, we have extended the low range of accessible frequencies by performing creep experiments at permissible temperatures (110 °C for the PG series) and converting the time-dependent compliance data to frequency-dependent moduli.[33] In this regard, a stress-controlled rheometer Physica MCR-501 (Anton Paar, Austria) was utilized. Invar parallel plates of 8 mm diameter and sample gap in the rage 0.6−1 mm were used. Temperature control of ±0.1 °C was achieved with a Peltier system under a nitrogen atmosphere. In particular, compliance as a function of time was measured for all the samples in the linear regime. The latter was ensured by imposing low stress, as judged by the corresponding linear strain range. The results of these creep experiments have been converted into dynamic moduli G' and G'',[33,34] in order to extend the master curves from ARES to lower frequencies. This conversion may be performed by Fourier transformation. However, the actual application of those integral transformations to experimental data is not straightforward as it represents an ill-conditioned problem.[33,34] Alternatively, approximate numerical formulas for this purpose have been proposed long ago and proven to be robust.[35] Their advantage is that they do not involve any integration of the functions measured. We used these formulas to calculate G' and G'' as functions of frequency. Note that we did not perform any creep tests on the commercial samples because the terminal regime had already been reached via frequency sweeps.

Time−temperature superimposed viscoelastic moduli have been obtained by shifting all the data to the chosen reference temperature by using two-dimensional minimization. Whereas this choice is arguable, we note that the more appropriate (in our view) with vertical density compensation[32,36] requires exact knowledge of the temperature dependence of the density, which is not known for this type of complex architectural polymers. Nevertheless, as we discuss below the chosen method gave reliable and robust results.

II.4. Molecular Dynamics (MD) Simulations. Atomistic molecular models of PG1−PG4 were recently investigated.[29] Similar elongated backbone conformations, with an average length of ∼2.2 Å per repeating unit, were proposed for all four DPs, even though the stiffness was found to increase with the generation of the dendron. MD simulations of the four models were performed in vacuo using the NAMD program.[37] For this purpose a polymer chain involving 150 repeating units was considered for each system; the numbers of explicit atoms used to describe the PG1, PG2, PG3, and PG4 chains were 11 852, 27 152, 57 752, and 118 952, respectively.

Energy minimizations to eliminate unfavorable interactions were carried out using the conjugate gradient algorithm. MD simulations in the gas phase were performed heating up the system from 0 to 298 K using a rate of 1 K each 1.5 ps. Each production trajectory was 10 ns long, coordinates being saved every 5 × 104 steps (100 ps intervals) for subsequent analysis. The energy was calculated using the AMBER force field.[38] Bonding and van der Waals parameters were taken from generalized AMBER force field (GAFF).[39] Atomic charges were adjusted using the restrained electrostatic potential (RESP) strategy.[40] Atom-pair distance cutoffs were applied at 12 Å to compute van der

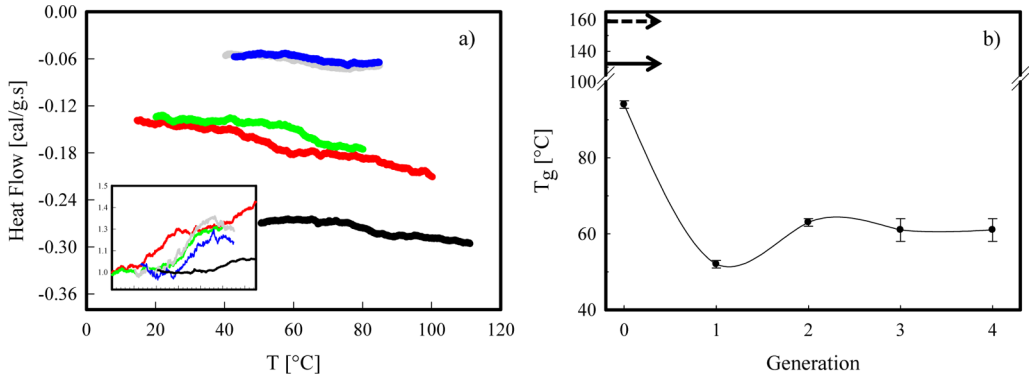

Figure 3. (a) DSC scans for the dendronized polymers: PG0, black; PG1, red; PG2, green; PG3, gray; PG4, blue. The inset is the normalized heat flow (see text for details) in the temperature range of the jump. (b) Glass transition temperatures as a function of generation for the dendronized polymers. The full and dashed arrows indicate the glass transition temperatures of PMMA and PtBMA, respectively.

Waals and electrostatic interactions. Bond lengths involving hydrogen atoms were constrained using the SHAKE algorithm with a numerical integration step of 2 fs.[41]

III. RESULTS AND DISCUSSION

III.1. Glass Transition Temperature. Figure 3a illustrates the heat flow (divided by the weight of the sample) as a function of temperature for the various dendronized polymers. Each heat flow jump corresponds to the glass transition temperature which is reported in Figure 3b. The heat flow increases with decreasing generation, consistently. This means lower specific heat and smaller heat flow involved in the transition (see also the inset) for the higher generations. The higher generations are indeed less mobile due to higher branching and intermolecular hydrogen bonding. The inset in Figure 3a has been obtained by normalizing the relative heat flows by the mean initial heat value at low temperature for each generation. The breadth of the transition appears to increase with generation, conforming to respective data with similar systems.[5] Hence, dense branching and hydrogen bonding reduce the local mobility and hence affect the distribution of the local relaxation times and of course the glass transition. In Figure 3b, glass transition temperatures of the different generation are reported along with those of PMMA and PtBMA (full and dashed arrows, respectively). The PtBMa exhibits a significantly higher T_g compared to PMMA due to the steric effects of the *tert*-butyl group. The glass transition temperatures of both commercial samples are higher than the usual values in the literature. This finding is attributed to tacticity.[42] The samples are indeed mostly syndiotactic, as reported by the supplier (75−85% syndiotactic content). Concerning the dendronized polymer samples, they all exhibit lower T_g compared to the two commercial linear samples. Further, from PG0 to PG1, i.e., from one Boc(NH) group per monomer (sample PG0) to two Boc(NH) groups per monomer (PG1), there is an abrupt decrease of the glass transition temperature. We speculate that the open structure of PG0 promotes intermolecular hydrogen bonding, as also supported by the rheological data discussed below. Moreover, the pendant side group in PG1 increases the effective intramolecular free volume and thus the local mobility of the backbone main chain. As the generation number increases further, T_g increases slightly and eventually levels off. This increase of T_g by about 10 °C from generation PG1 to the others is unambiguous and remarkable, albeit weak, and reflects a slower local dynamics. We attribute it to the enhanced molecular crowdedness of these dendronized polymers with bulkier pendant side groups, as also supported by MD simulations discussed below.[29] It is tempting to draw analogies with conventional branched or hyperbranched polymers[43] although in the present case the segments between branch points are too short and have end groups involved in bonding. With this in mind, one can consider that, from a dynamic point of view, increasing generation means an increase in both the number of branching points and the number of dangling ends. The number of branching points yields denser local packing and a reduction in the overall mobility of the macromolecules; hence, it contributes to the enhancement of T_g; on the other hand, an increased number of free ends results in enhanced mobility, and hence it contributes to a decrease of T_g. At the same time, hydrogen bonds, which depend on generation, enhance T_g.[44] This naive, albeit reasonable, qualitative assessment suggests that the dependence of the glass transition temperature on generation is not trivial. Nevertheless, our results are in complete agreement with previous theoretical treatment[22] and experiments.[23] Indeed, it has already been shown that during dendritic growth T_g approaches a final value, and no significant changes are found after approximately the fourth generation. There is of course an analogy with the well-known saturation of T_g as a function of molar mass for linear polymers.[45] Here, we found saturation of T_g already after the second generation. This also appears in qualitative agreement with results for similar dendronized polymers (although with much different degrees of polymerization between generations), which indicate an increase of T_g with dendron generation up to the second generation;[5] however, the trend of increasing T_g was slightly different, and the fourth generation was reported to have an unexpectedly low T_g, possibly due to a much lower degree of polymerization. Fine molecular details and polydispersity of different generations could also play a role. We emphasize that an important advantage of our present polymers is that the degree of polymerization is almost constant throughout the different generations, which enables a systematic study of properties (such as the glass transition temperature) as a function of generation. Moreover, it appears from the data that in the temperature range studied the hydrogen bonds remain stable, again in agreement with literature.[5] On the other hand, their local motion has different temperature dependence from the local one, and their coupling is different for different generation and reflected on the heat flow and the rheology (below).

dx.doi.org/10.1021/ma301029t | *Macromolecules* 2012, 45, 8813−8823

III.2. Linear Viscoelastic Response. In this section we shall present the master curves of shifted viscoelastic moduli for the series of dendronized polymers as a function of shifted frequency. These results were obtained by combining SAOS data at different temperatures and creep data which were converted to the frequency domain, as discussed in section II.3. Before proceeding with the frequency spectra, however, a note on the strain amplitudes used in SAOS is in order. Typical dynamic strain sweep results for DP samples are depicted in Figure 4. All generations exhibit linear response in the

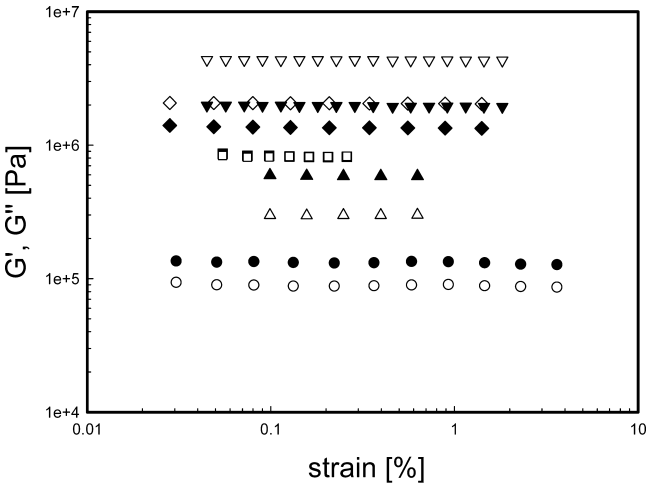

Figure 4. Strain sweep experiments at reference temperature 110 °C and frequency 100 rad/s. PG0: G' (○), G''(●); PG1: G' (△), G'' (▲); PG2: G' (□), G'' (■); PG3: G' (◇), G'' (◆); PG4: G' (▽), G'' (▼).

examined strain range. This means that the range 0.1%−1% strain is appropriate for performing SAOS. Note that at this frequency the zeroth and first generations exhibit liquid-like behavior ($G'' > G'$), whereas the second generation marks the transition to solid-like behavior ($G' \geq G''$), which becomes more evident with increasing generation number.

The starting point is the linear response of the linear polymers, which serves as reference. Figure 5 depicts the master curves of PG0 and the two linear PMMA and PtBMA samples. The comparison has been made at the same distance from T_g. Based on the discussion on glass transition, this does not guarantee isofrictional conditions (see below), but on the other hand, it offers a good reference for comparing the data as we show below. Note that detecting the exact isofrictional conditions does not affect the results and message of this work and is beyond its scope. The relative temperatures are indicated in the caption of Figure 5. On the other hand, the high-frequency crossover of the moduli is essentially identical for the entangled PMMA and PtBMA polymers. This crossover is related to the inverse Rouse time of an entanglement segment, being proportional to segmental friction coefficient.[1,46] It is not always easy to probe it univocally due to the low temperatures (close to the glass transition temperature) needed to measure. Its determination can then be affected by the local relaxation. The situation is even more complicated for PG0, a linear chain with Boc(NH) side groups attached to each monomer of the main chain (see Figure 2). The presence of hydrogen bonds, in particular intermolecular ones, which are temperature-dependent, makes the determination of the isofrictional conditions nontrivial. Moreover, this polymer

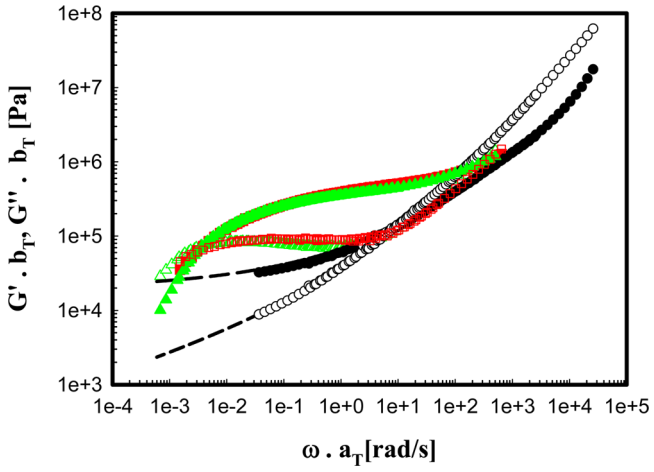

Figure 5. Master curves of the linear viscoelastic behavior for the two commercial samples and the PG0 at T-T_g=40 °C. The relative temperatures are: PG0:134 °C; PMMA: 170 °C; PtBMA: 200 °C. PG0: G' (●), G'' (○); PMMA: G' (■), G'' (□); PtBMA: G' (▲), G'' (△). Lines are converted creep data (see text).

does not display the typical rheological behavior of entangled linear polymers in the experimental frequency window. Its open structure promotes intermolecular hydrogen bonding, and its rheology conforms to its higher T_g. Moreover, the low-frequency regime, which has been reached via conversion of the creep test into the viscoelastic regime, reflects the behavior of a stiff, network-like material. Again, we argue that this behavior is due to the presence of the Boc(NH) groups along the main chain, which greatly reduce the mobility of the backbone via steric hindrance and intermolecular hydrogen bonding. In addition, π,π-stacking between benzene groups is also possible, but it is much weaker than hydrogen bonding. Nevertheless, we note that rheology cannot quantify the contribution of each of these types of molecular interactions to the overall viscoelastic response of the examined polymers.[47] The plateau modulus of PG0 (G' lower frequencies) is about 1 decade smaller than that of PMMA and PtBMA, suggesting that the stress-carrying element, typically the molar mass of the effective strand between junctions, is larger by 1 order of magnitude. Therefore, it is evident from the above that PG0 is not typical entangled polymer and will not be considered as such below. On the other hand, the two entangled linear polymers PMMA and PtBMA exhibit the expected response with an intermediate plateau and low-frequency terminal regions. Moreover, from the dynamic rheological data of Figure 5 (value of plateau modulus G_N^0), the molar masses between entanglements $M_e = 4\rho RT/5G_N^0$ (with ρ the density and R the gas constant) are estimated for these two commercial polymers and found to be very similar (M_e = 7200 g/mol for PMMA and M_e = 8320 g/mol for PtBMA). This suggests that, given the very similar molar masses M_w (see Table 1), the rheological response of PMMA and PtBMA should be almost indistinguishable at the same distance from T_g. Indeed, Figure 5 confirms this suggestion.

Figure 6 depicts the master curves of frequency linear viscoelastic moduli for the dendronized polymers at two different distances above T_g, 40 and 80 °C. Although at $T - T_g$ = 40 °C the curves are almost overlaying on each other, the comparison is not isofrictional. In addition to the discussion in section III.1, this is further confirmed by the different location of the master curves of the dendronized polymers at the

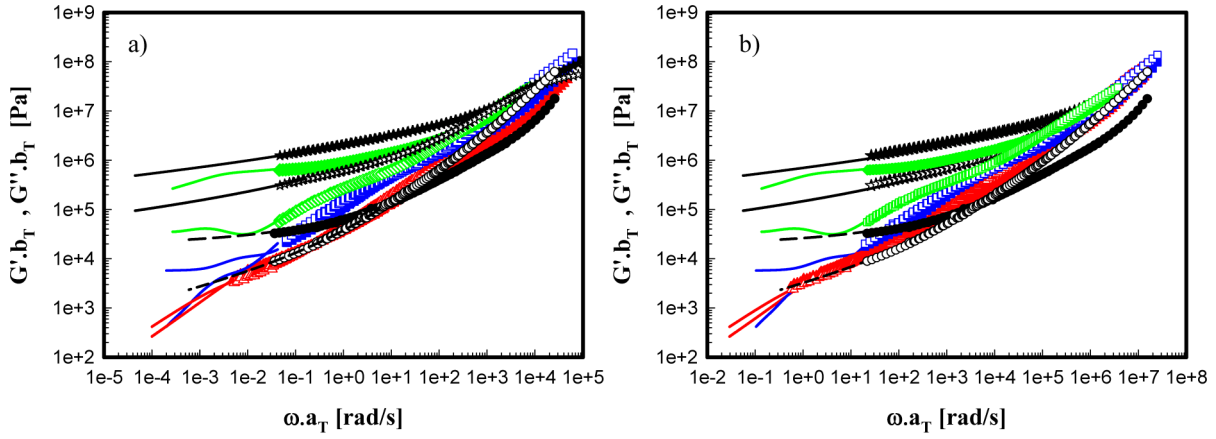

Figure 6. Master curves of the linear viscoelastic moduli of the dendronized polymer samples at reference temperatures of $T = T_g + 40$ °C (a) and $T = T_g + 80$ °C (b). The relative temperatures are for (a) PG0: 134 °C; PG1: 92 °C; PG2: 103 °C; PG3: 101 °C; PG4: 101 °C. For (b): PG0: 174 °C; PG1: 132 °C; PG2: 143 °C; PG3: 141 °C; PG4: 141 °C. PG0: G' (●), G'' (○); PG1: G' (▲), G'' (△); PG2: G' (■), G'' (□); PG3: G' (◆), G'' (◇); PG4: G' (★), G'' (☆). Lines are converted moduli from creep data (see text): PG0 (- - -); PG1 (red); PG2 (blue); PG3 (green); PG4 (black).

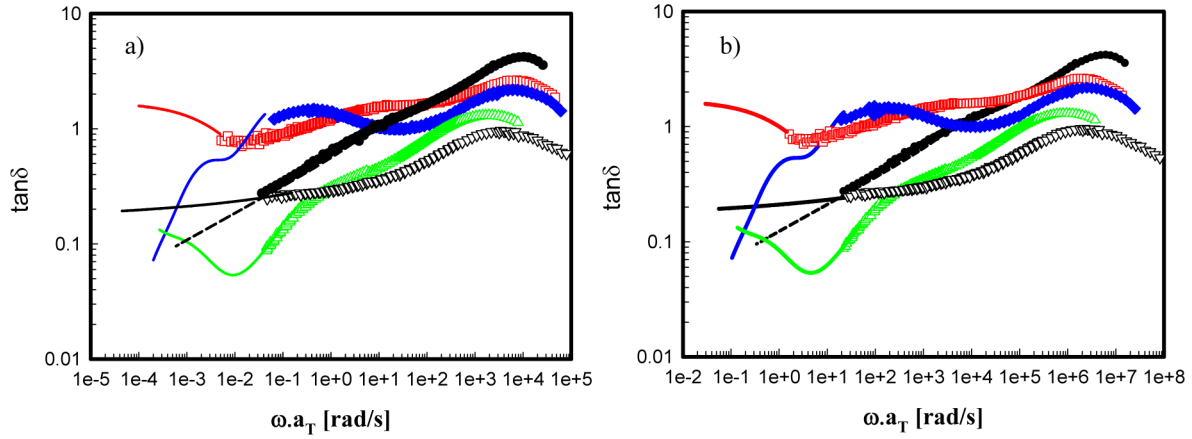

Figure 7. Time−temperature superimposed tanδ as a function of frequency at reference temperatures of $T = T_g + 40$ °C (a) and $T = T_g + 80$ °C (b). PG0: ●; PG1: □; PG2: ◆; PG3: ▲; PG4: ▽. Lines are converted moduli from creep data (see text).

different distance $T - T_g = 80$ °C, shown in Figure 6b, in particular regarding PG0. This indeed indicates that the local friction deduced from the WLF equation[32] is not the monomeric friction but an apparent one. This reflects the presence of additional mechanism restricting local mobility such as hydrogen bonding. Therefore, the interpretation of the temperature-dependent relaxation of the dendronized polymers is not a straightforward WLF-based analysis as in simply amorphous homopolymers and should be done with care (see also section III.3).

It is instructive to observe the viscoelastic response also in the form of frequency-dependent tangent of the loss angle, tanδ = G''/G', where for example the low-frequency responses distinguish the different generations, as seen in Figure 7. PG2 and PG3 exhibit a solid-like response since $G' > G''$, but in both cases the shape of the moduli (Figure 6) and tanδ curves (with clear minimum in G'' for PG3) are suggestive of a multimode relaxation spectrum, attributed to the slightly different internal conformations and molecular flexibility.[29] Moreover, it is even more evident from Figure 7 that the relative location of master curves in the plot is not invariant to the choice of reference temperature.

The low-frequency regime (lines in Figure 6) was specifically assessed in order to elucidate the differences among generations and in particular examine whether the higher generations samples reached terminal relaxation. Creep measurements enabled extending the frequency range by more than 2 decades. As the generation of the dendronized polymers increases, the behavior of the DPs at lower frequencies changes monotonically and in fact varies from liquid-like (PG1) to solid-like response (PG4). Note that the plateau modulus of PG0 has much lower value than those of PG3 and PG4. On the other hand, PG0 is not really a DP, and hence hereafter we shall not compare its viscoelastic response against that of the DPs. We note that for PG1 and PG2 the dynamic moduli are nearly equal over several decades of intermediate to high frequencies, and they appear to follow a power law with a slope of about 0.5. PG1 is the only structure exhibiting terminal relaxation in the examined frequency window. PG2 and PG3 exhibit in the low-frequency regime a viscoelastic response characterized by a plateau G' (or weak frequency dependence by $G' \gg G''$) and a range of internal relaxation modes as judged by the shape of the loss modulus G''. On the other hand, the behavior of PG4 is very different. The dominant response over about 7 decades in frequency is solid-like with G' exceeding G'' and being nearly parallel, exhibiting eventually a very weak frequency dependence (a slope of about 0.2). This finding is suggestive of gel-like

dx.doi.org/10.1021/ma301029t | Macromolecules 2012, 45, 8813−8823

response and reminiscent of the percolation observed in hyperbranched systems.[46] What is important is that after local relaxation at high frequencies the system immediately follows this gel-like response. There is no evidence of internal faster relaxation as in PG1 and PG2. Hence, the picture emerging from the rheological data suggests that the linear viscoelastic response of the DPs has nothing to do with the classic entanglement dynamics[11−14] and should be controlled by intermolecular interactions which depend on generation. Actually, the topological constraints at the scale of the DPs as mentioned in the context of the "sausage" picture (Figure 1) and the two types of bonds and in particular the hydrogen bonds seem responsible. With increasing generation number, the rheological response suggests the appearance of a stronger network. Increased interchain hydrogen-bonding density and branch point density (see also discussion below) seem responsible for this peculiar rheological response. Of course, the overall rheological picture suggests a possible molecular mechanism, but it is not sufficient for a definitive explanation. The link between branching density and hydrogen bond distribution and hence to the enhanced probability of intermolecular bonding for the higher-generation polymers is in our opinion at the origin of the viscoelastic response.

The above scenario for DPs is examined and elucidated by MD simulations. The results provide detailed information on the molecular conformation of DPs of different generations.[29] They confirm the elongated structures ("sausages") and enhanced rigidity and thickness with generation. These features are reflected in Figure 8, which depicts representative atomistic

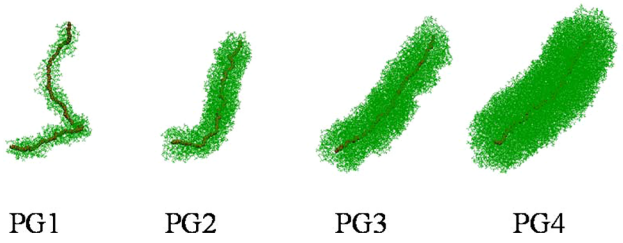

Figure 8. Atomistic models derived from MD simulations[29] for the DPs PG1−PG4. The backbone atoms are represented using purple thick spheres. The cylindrical (i.e., sausage-like) shape and the increment of the thickness with the generation are clearly evidenced.

models of PG1−PG4. This is consistent also with AFM and SANS studies in solution.[8,27,49] In fact, the estimated constant-density elongated-core radius (referring to Figure 8) of the DPs from SANS measurements in dilute solution is 1.67, 2.17, 2.92, and 3.85 for PG1, PG2, PG3, and PG4, respectively.[49] More importantly, the calculated density profiles reveal important information on the internal structure. Figure 9 depicts the density of the DPs as a function of the distance to the backbone measured using the vector perpendicular to the helix-axis, i.e., the effective "sausage" radius. We observe that for large distance r the density is high (1.1−1.2 g/cm^3) and nearly constant, and eventually it drops until cancellation. The fraction of r corresponding to the high constant density signifies dense intramolecular packing in the form of a rigid object, here almost cylindrical (the "sausage"). On the other hand, the fraction of decreasing density corresponds to looser packing and suggests the possibility of interpenetration from neighboring molecules in the melt state. Hence, the present DPs can be considered as effective (elongated) core−shell particles (cylinders). Since the

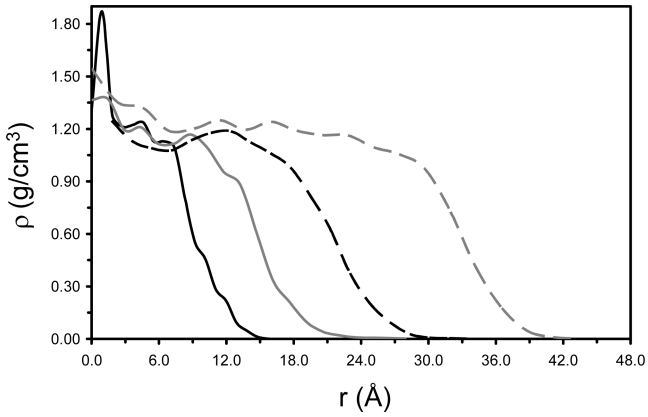

Figure 9. Density profile for PG1−PG4 representing the density (ρ) against the distance to the backbone measured using the vector perpendicular to the helix axis (r): PG1 (black —); PG2 (gray —); PG3 (black - - -); PG4 (gray - - -). The profile displayed for each DP corresponds to an average considering different cross sections within a given snapshot and different snapshots.

r fraction of interaction (r region of decreasing density over the whole r region in Figure 9) is diminishing as generation increases, these core−shell cylinders become effectively crew-cut.[50] There is analogy with simpler spherical core−shell spherical particles and in particular multiarm star polymers, where the density profile shows the regions of interpenetration which depend on functionality, as demonstrated by simulations and scattering experiments.[48] Therefore, as generation increases, there is a combination of topological "sausage" interaction and intermolecular bonding. Figure 10 depicts the

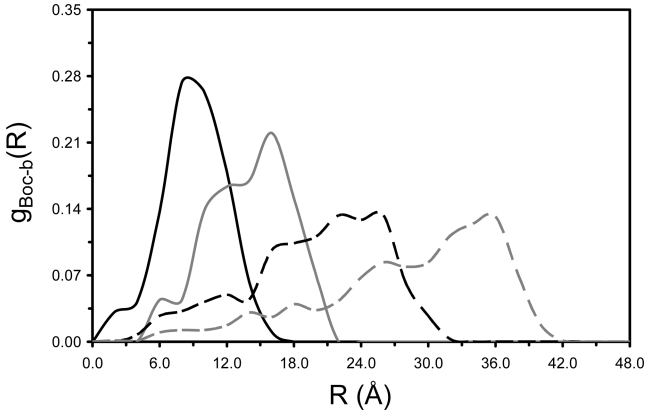

Figure 10. Distribution of the Boc groups, gBoc-b, as a function of the distance from the backbone (R) for PG1−PG4: PG1 (black —); PG2 (gray —); PG3 (black - - -); PG4 (gray - - -).

calculated distribution of Boc groups as a function of the lateral distance from the backbone for the different DPs. It is evident that as generation increases, the peak of the distribution increases toward the periphery. In conjunction with the density profile, this important result suggests that as generation increases, there are more intermolecular bonds formed, and this explains the increase of the plateau modulus (and overall change of viscoelastic behavior) from PG1 to PG4. For PG1, in particular, the Boc groups are so close to the backbone that there intermolecular bonding is unlikely, and hence the molecular eventually exhibits terminal relaxation.

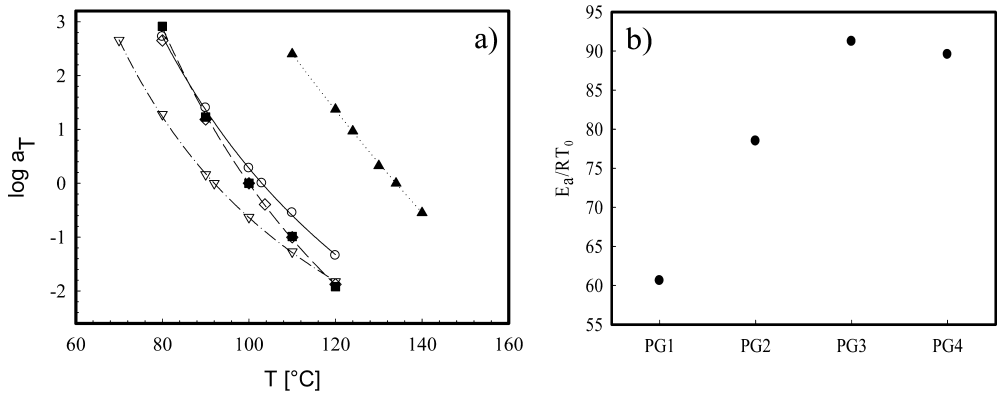

Figure 11. (a) Temperature-dependent horizontal shift factors for the various polymers used in this work. The lines are WLF fits through the data. PG0: ▲; PG1: ▽; PG2: ○; PG3: ■; PG4: ◇. (b) Normalized activation energies for DPs as a function of generation number ($T_0 = T_g + 40$ °C).

Table 2. Parameters from WLF Fit for the Dendronized Polymers

samples	T_g [°C]	c_1 ($T_0 - T_g = 40$ °C)	c_2 ($T_0 - T_g = 40$ °C) [°C]	$c_{1g,40}$	$c_{2g,40}$ [°C]	c_1 ($T_0 = 110$ °C)	c_2 ($T_0 = 110$ °C) [°C]	$c_{1g,110}$	$c_{2g,110}$ [°C]
PG0	94	30.5	328.3	34.7	288.3	19	169.2	20.9	153.2
PG1	52	6.99	79.7	14.0	39.7	6.3	102.5	14.4	44.5
PG2	63	9.1	99.3	15.3	60.8	11.8	145.2	17.3	98.2
PG3	61	10.7	95.7	18.4	55.7	11.7	124.8	18.8	78.8
PG4	61	9.4	87.6	17.3	47.6	13.9	148.8	20.7	99.8

To provide additional support to the above scenario, we performed a simple qualitative test. We attempted at diluting the macromolecules in toluene, which is an apolar solvent and hence is not expected to influence the hydrogen bonds formed. Interestingly, PG1 dissolves easily whereas higher generation DPs do not. In our opinion, this is suggestive of predominantly intramolecular bonding in PG1 and intermolecular bonding in the higher generations. Expectedly, PG0 was also insoluble in toluene.

The idea that hydrogen bonding enhances the plateau modulus is of course not new.[15,51] Moreover, here we have a far more complicated situation due to the complex topology of the DPs. Topological constraints other than classic entanglements can enhance the plateau modulus, as for example in the case of microgel systems in the melt.[52] However, the interpretation offered here suggests that the DPs are very different. Microgels consist of hyperbranched architectures which are colloidal in nature. By changing the dimensions of the microgels, it is possible to tailor the rheological response, a feature shared by DPs as well. In the limit of large sizes (above 20 nm), controlled at chemistry level, spherical polystyrene microgels exhibited elastic response at low frequencies.[52] Their low-frequency response (G' plateau exhibiting high values) was qualitatively similar to our dendronized samples PG3 and PG4. However, these microgels had no bonding interactions, and their low-frequency behavior (plateau modulus and very slow relaxation) was suggestive of particle-like colloidal response in the melt state due to excluded volume effects at the size scale of the whole particle; hence, it is important for large particles, similar to that observed in multiarm star polymers as well.[48]

III.3. Temperature Dependence of the Dynamic Response. As already mentioned, the presence of hydrogen bonding complicates the interpretation of the temperature-dependent dynamics. Starting with the WLF equation,[32] it is usually possible to determine the parameters on an iso-free-volume basis. This type of analysis was utilized by Farrington et al. in examining dendritic poly(benzyl ether)[43] and by Dorgan et al. for dendritically branched polystyrene.[4] However, with the present samples this approach has several drawbacks as discussed in the context of Figure 6 above. Figure 11a depicts the temperature shift factors for the various dendronized polymers with different relative reference temperature. The distance from T_g for all the samples is 40 °C. This distance has been chosen based on the accessibility of the relative temperatures for all the samples. The data were fitted with the WLF equation[32] $\log a_T = (-c_1(T - T_0))/(c_2 + T - T_0)$, and c_1 and c_2 were estimated from the fits and are reported in Table 2.

The trend with temperature of a_T reflects the differences in the glass transition temperature for the different generations and is in reasonable agreement with the leveling-off of the sample's glass transition temperature for generations PG2 and higher (Figure 3b). It is worth noting that the shift factor curves exhibit a steeper temperature dependence for PG3 and PG4 in comparison to PG1 and PG2, as observed in the low-temperature regime in Figure 11a. This appears to conform to the predominance of intermolecular hydrogen bonding at higher generations.[44] In fact, Figure 11b depicts the normalized activation energy (E_a/RT_0) of the DPs, as estimated from an Arrhenius fit of the respective high-temperature shift factor data at $T_0 = T_g + 40$ °C. Despite the error involved in such an analysis, the unambiguous increase of E with generation number, leveling off at PG4, confirms indeed the increasing importance of hydrogen bonding.

The WLF coefficients c_1 and c_2 can be converted to the values c_{1g} and c_{2g} at the glass transition temperature using the following equations:[32,43]

$$c_{1g} = \frac{c_1 c_2}{c_2 + T_g - T_0}$$
$$c_{2g} = c_2 + T_g - T_0 \quad (1)$$

Table 2 reports c_1 and c_2 at $T_0 - T_g = 40$ °C calculated from the fits in Figure 11a and the corresponding c_{1g} and c_{2g} values

dx.doi.org/10.1021/ma301029t | Macromolecules 2012, 45, 8813−8823

obtained from eqs 1. Alternatively, we have also evaluated c_1 and c_2 at a common reference temperature of 110 °C, and by using eqs 1 we have attempted at verifying the values of c_{1g} and c_{2g}. A subscript (temperature) has been added to facilitate the reader. The following conclusions can be drawn from Table 2: if one looks at the values of c_{1g} and c_{2g} for the dendronized polymers, the difference for the different generations at T_g clearly demonstrates that the polymers are not compared at truly isofrictional conditions. Moreover, the different values of c_{1g} and c_{2g} depending on the different temperature taken as reference for the evaluation of c_1 and c_2, namely $T_0 - T_g = 40$ and 110 °C in this case, indicate that the WLF fit changes shape according to reference temperature, in contrast to the behavior of amorphous homopolymers. We believe that the lifetime of the hydrogen bonds (which we do not know precisely) is making the difference. Their role has already been discussed in the context of DSC and rheology. In addition, the fact that the c_{1g} and c_{2g} values of PG1 are very close corroborates this argument as in this dendronized polymer the hydrogen bond contribution is the weakest (see discussion of rheological and measurements and MD simulations above). Therefore, it is not particularly meaningful to extract fractional free volumes at the glass transition temperature from the WLF fit coefficients.

Molecular dynamic simulations help to resolve the issue of calculating the free volume at the glass transition temperature by evaluating the "unoccupied volume" (V_u),[53] which refers here to empty space existing between the van der Waals spheres used to describe the molecules. It has been calculated using the atomistic models of PG1−PG4 derived from MD simulations at 298 K (Figure 7). The fraction of empty space predicted for PG1, PG2, PG3, and PG4 is 0.58, 0.48, 0.50, and 0.46, respectively. This is confirming that the structures are becoming more crowded with generation and that the abrupt decrease of the fraction of empty space happens between PG1 and PG2.

Figure 12 represents the variation of V_u as a function of the distance to the backbone measured using the vector perpendicular to the helix axis. The profiles obtained for PG2, PG3, and PG4 are relatively similar, whereas the profile of PG1 shows a more abrupt fluctuation in the intermediate region and a slightly more marked transition toward the unity in the external layer of the cylinder. These behaviors have been attributed to the fact that the molecular stiffness increases with the generation.

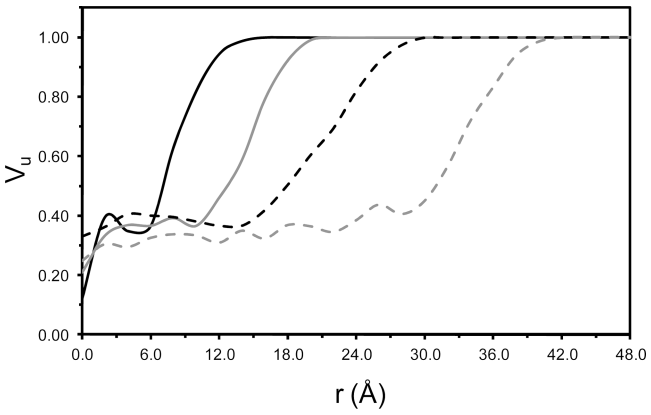

Figure 12. Unoccupied volume (V_u) calculated for PG1−PG4 against the distance to the backbone measured using the vector perpendicular to the helix axis (r): PG1 (black —); PG2 (gray —); PG3 (black - - -); PG4 (gray - - -). The models derived from MD simulations at 298 K (Figure 7) were used for these calculations.

IV. CONCLUDING REMARKS

In this work we have investigated the linear viscoelastic properties of well-defined dendronized polymers in the bulk. These ultrahigh-molar-mass polymeric structures consist of polymethacrylate backbones, where each monomer is linked to a dendron of varying generation, from zeroth PG0 to fourth PG4. The degree of polymerization is almost constant throughout the different generations, which enables a systematic study of properties in bulk as a function of generation. The glass transition temperature was found to decrease with generation up to PG1, and to level off for the higher generations. This behavior was attributed to the effects of dangling ends, local packing, and bonding due to Boc groups and aromatic benzene groups. This is confirmed also by the decrease of the heat flow and its broadening with increasing generation. The coupling of segmental friction and hydrogen bonding, in particular, renders the analysis of the linear viscoelastic master curves nontrivial and calls for further investigations of these complicated macromolecules.

The systematic rheological studies revealed an unusual viscoelastic response. It appears that DPs exhibit elongated core−shell conformations, and the combination of topological interactions at the scale of the molecule ("sausage"-like) and intermolecular bonding, a picture supported by MD simulations, controls their dynamics. As the generation increases, there is a transition from viscoelastic liquid (PG1) to viscoelastic solid, the latter having enhanced plateau modulus from PG2 to PG4. In addition, PG0, which is not a DP but could be considered as a precursor, exhibits solid like response attributed to intermolecular hydrogen bonding.

Dendronized polymers offer the unique advantage of large size and ultrahigh molar mass and wide-ranging tunability and functionalization. Moreover, the nearly constant degree of polymerization of different generations is important for appreciating the importance of the local packing effects.

Hence, it is now possible to obtain ultrahigh molar mass functional polymers with great versatility in terms of applications and tailored rheology at molecular level. By simply shifting generations, the response alters from polymeric fluid-like to solid-like. The MD results obtained support this picture and hold the premise for further elucidating the dynamics of this intriguing class of macromolecules.

AUTHOR INFORMATION

Corresponding Author

*E-mail rossana@iesl.forth.gr.

Notes

The authors declare no competing financial interest.

ACKNOWLEDGMENTS

We are grateful to Ulrich Jonas, Moshe Gottlieb, and Frank Snijkers for useful discussions and Christian Coppola for allowing us to perform preliminary creep measurements in the laboratories of Versalis, Ravenna, Italy. C.A. and O.B. are indebted to CESCA for computational facilities. Partial support has been received by the EU (ITN DYNACOP, grant 214627), the Swiss National Science Foundation (SNSF), NRP 62 (Smart Materials), MICINN (MAT2009-09138 with FEDER

funds), and the Generalitat de Catalunya (2009SGR925 and "ICREA Academia" prize for excellence in research to C.A.).

REFERENCES

(1) McLeish, T. C. B. *Adv. Phys.* **2002**, *51*, 1379−1527.
(2) Newkome, G. R.; Moorefield, C. N.; Vögtle, F. *Dendritic Molecules: Concepts, Synthesis, Perspectives*; Wiley-VCH: Weinheim, 1996.
(3) Hu, M.; Xia, Y.; Mckenna, G. B.; Kornfield, J. A.; Grubbs, R. H. *Macromolecules* **2011**, *44*, 6935−6943.
(4) Dorgan, J. R.; Knauss, D. M.; Al-Muallem, H. A.; Huang, T.; Vlassopoulos, D. *Macromolecules* **2003**, *36*, 380−388.
(5) Zhang, A.; Okrasa, L.; Pakula, T.; Schlüter, A. D. *J. Am. Chem. Soc.* **2004**, *126*, 6658−6666.
(6) Vögtle, F.; Gestermann, S.; Hesse, R.; Schwierz, H.; Windisch, B. *Prog. Polym. Sci.* **2000**, *25*, 987−104.
(7) Zhang, A.; Zhang, B.; Wächtersbach, E.; Schmidt, M.; Schlüter, A. D. *Chem.—Eur. J.* **2003**, *9*, 6083−6092.
(8) Zhang, B.; Wepf, R.; Fischer, K.; Schmidt, M.; Besse, S.; Lindner, P.; King, T. B.; Sigel, R.; Schurtenberger, P.; Talmon, Y.; Ding, Y.; Kröger, M.; Haplerin, A.; Schlüter, A. D. *Angew. Chem., Int. Ed.* **2011**, *50*, 737−740.
(9) Nystrom, A. M.; Furo, I.; Malmstrom, E.; Hult, A. *J. Polym. Sci., Part A: Polym. Chem.* **2005**, *43*, 4496−4504.
(10) Andreopoulou, A. K.; Carbonnier, B.; Kallitsis, J. K.; Pakula, T. *Macromolecules* **2004**, *37*, 3576−3587.
(11) McLeish, T. C. B. *Europhys. Lett.* **1988**, *6*, 511−516.
(12) Read, D. J.; Auhl, D.; Das, C.; den Doelder, J.; Kapnistos, M.; Vittorias, I.; McLeish, T. C. B. *Science* **2011**, *333*, 1871−1874.
(13) van Ruymbeke, E.; Orfanou, K.; Kapnistos, M.; Iatrou, H.; Pitsikalis, M.; Hadjichristidis, N.; Lohse, D. J.; Vlassopoulos, D. *Macromolecules* **2007**, *40*, 5941−5952.
(14) Watanabe, H.; Matsumija, Y.; van Rumbeyke, E.; Vlassopoulos, D. *Macromolecules* **2008**, *41*, 6110−6124.
(15) Stadler, R. *Prog. Colloid Polym. Sci.* **1987**, *75*, 140−145.
(16) de Greef, T. F. A.; Meijer, E. W. *Nature* **2008**, *453*, 171−173.
(17) Uppuluri, S.; Keinath, S. E.; Tomalia, D. A.; Dvornic, P. R. *Macromolecules* **1998**, *31*, 4498−4510.
(18) Samadi, F.; Wolf, B. A.; Guo, Y.; Zhang, A.; Schlüter, A. D. *Macromolecules* **2008**, *41*, 8173−8180.
(19) Namba, S.; Tsukahara, Y.; Kaeriyama, Y.; Okamoto, K.; Takahashi, M. *Polymer* **2000**, *41*, 5165−5171.
(20) Vlassopoulos, D.; Fytas, G.; Loppinet, B.; Isel, F.; Lutz, P.; Benoit, H. *Macromolecules* **2000**, *33*, 5960−5969.
(21) Pakula, T.; Zhang, Y.; Matyjaszewski, K.; Lee, H.; Boerner, H.; Qin., S.; Berry, G. *Polymer* **2006**, *47*, 7198−7206.
(22) Stutz, H. *J. Polym. Sci., Part B: Polym. Phys.* **1995**, *33*, 333−340.
(23) Wooley, K. L.; Hawker, C. J.; Pochan, J. M.; Fréchet, J. M. J. *Macromolecules* **1993**, *26*, 1514−1519.
(24) Stutz, H.; Illers, K. H.; Mertes, J. *J. Polym. Sci., Part B: Polym. Phys.* **1990**, *28*, 1483−1498.
(25) Guo, Y.; van Beek, J. D.; Zhang, B.; Colussi, M.; Walde, P.; Zhang, A.; Kröger, M.; Halperin, A.; Schlüter, A. D. *J. Am. Chem. Soc.* **2009**, *131*, 11841−11854.
(26) Roeser, J.; Moingeon, F.; Heinrich, B.; Masson, P.; Arnaud-Neu, F.; Rawiso, M.; Méry, S. *Macromolecules* **2011**, *44*, 8925−8935.
(27) Zhang, B.; Wepf, R.; Kröger, M.; Halperin, A.; Schlüter, A. D. *Macromolecules* **2011**, *44*, 6785−6792.
(28) Barner, J.; Mallwitz, F.; Shu, L.; Schlüter, A. D.; Rabe, J. P. *Angew. Chem., Int. Ed.* **2003**, *42*, 1932−1935.
(29) Bertran, O.; Zhang, B.; Kröger, M.; Halperin, A.; Schlüter, A. D.; Alemán, C., accepted.
(30) Becht, J.-M.; Meyer, O.; Helmchen, G. *Synthesis* **2003**, *18*, 2805−2810.
(31) Kuroda, K.; DeGrado, W. F. *J. Am. Chem. Soc.* **2005**, *127*, 4128−4129.
(32) Ferry, J. D. *Viscoelastic Properties of Polymers*, 3rd ed.; Wiley: New York, 1980.
(33) He, C.; Wood-Adams, P.; Dealy, J. M. *J. Rheol.* **2004**, *48*, 711−724.
(34) Evans, R. M. L.; Tassieri, M.; Auhl, D.; Waigh, T. A. *Phys. Rev. E* **2009**, *80*, 012501−1.
(35) Schwarzl, F. R. *Rheol. Acta* **1969**, *8*, 6−17.
(36) Kapnistos, M.; Vlassopoulos, D.; Roovers, J.; Leal, L. G. *Macromolecules* **2005**, *38*, 7852−7862.
(37) Phillips, J. C.; Braun, R.; Wang, W.; Gumbart, J.; Tajkhorshid, E.; Villa, E.; Chipot, C.; Skeel, R. D.; Kale, L.; Schulten, K. *J. Comput. Chem.* **2005**, *26*, 1781−1802.
(38) Cornell, W. D.; Cieplak, P.; Bayly, C. I.; Gould, I. R.; Merz, K. M.; Ferguson, D. M.; Spellmeyer, D. C.; Fox, T.; Caldwell, J. W.; Kollman, P. A. *J. Am. Chem. Soc.* **1995**, *117*, 5179−5197.
(39) Wang, J.; Wolf, R. M.; Caldwell, J. W.; Case, D. A. *J. Comput. Chem.* **2004**, *15*, 1157−1174.
(40) Cieplak, P.; Cornell, W.; Bayly, C.; Kollman, P. A. *J. Comput. Chem.* **1995**, *16*, 1357−1377.
(41) Ryckaert, J. P.; Ciccotti, G.; Berendsen, H. J. C . *J. Comput. Phys.* **1977**, *23*, 327−341.
(42) Biros, J.; Larina, T.; Trekoval, J.; Pouchly, J. *Colloid Polym. Sci.* **1982**, *260*, 27−30.
(43) Farrington, P. J.; Hawker, C. J.; Fréchet, J. M. J.; Mackay, M. E. *Macromolecules* **1998**, *31*, 5043−5050.
(44) Vukovic, J.; Jovanovic, S.; Lechner, M. D.; Vodnik, V. *J. Appl. Polym. Sci.* **2009**, *112*, 2925−2934.
(45) Fox, T. G.; Flory, P. J. *J. Appl. Phys.* **1950**, *21*, 581−591.
(46) Rubinstein, M.; Colby, R. H. *Polymer Physics*; Oxford University Press: New York, 2003.
(47) Rosen, S. L. *Fundamental Principles of Polymeric Materials*; Wiley: New York, 1993.
(48) Pakula, T.; Vlassopoulos, D.; Fytas, G.; Roovers, J. *Macromolecules* **1998**, *31*, 8931−8940.
(49) Sigel, R.; Schurtenberger, P.; Schlütter, A. D. Unpublished data, 2012.
(50) Halperin, A.; Tirrel, M.; Lodge, P. *Adv. Polym. Sci.* **1992**, *100*, 31−71.
(51) Tobolsky, A. V.; Shen, M. C. *J. Phys. Chem.* **1963**, *67*, 1886−1891.
(52) Antonietti, M.; Pakula, T.; Bremser, W. *Macromolecules* **1995**, *28*, 4227−4233.
(53) Curcó, D.; Zanuy, D.; Alemán, C. *J. Comput. Chem.* **2003**, *24*, 1208−1214.